

Section 3

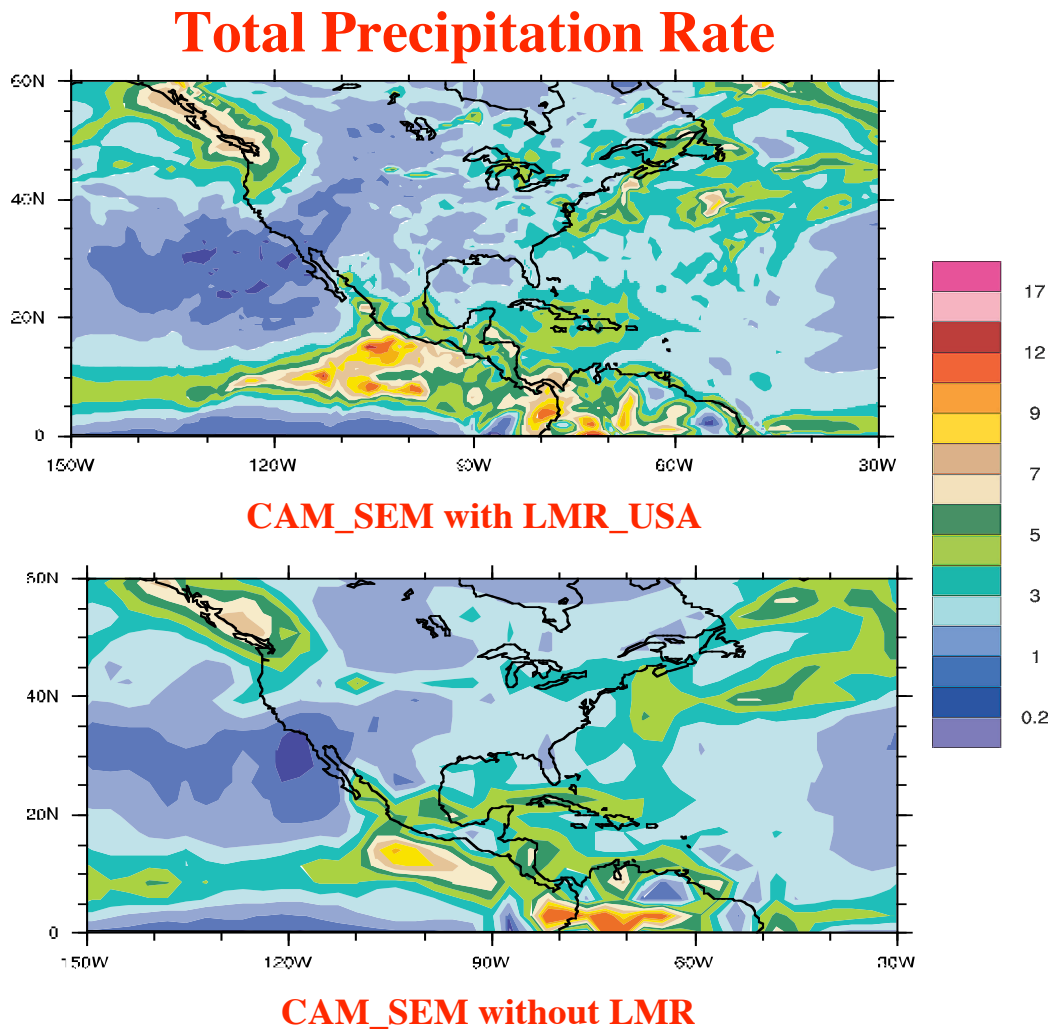
Computational studies including new techniques, the effect of varying model resolution, parallel processing

CLIMATE MODELING WITH SPECTRAL ELEMENTS

Ferdinand Baer, Dept. of AOSC, U. of Maryland, College Park, MD 20742
Houjun Wang, Dept. of AOSC, U. of Maryland and NCAR
Joseph J. Tribbia, NCAR
Aimé Fournier, NCAR

Toward improving climate model-component performance and accuracy, we have developed an atmospheric component climate model entitled the Spectral Element Atmospheric Climate Model and denoted it as (CAM_SEM). CAM_SEM includes a unique dynamical core, previously reported as SEAM (Spectral Element Atmospheric Model), and we have now coupled it to the physics component of the Community Atmosphere Model (CAM) as well as its land surface component (CLM) available from NCAR. We have also included in this model the capability for local mesh refinement to seamlessly study imbedded higher-resolution regional climate concurrently with the global climate. Additionally, the numerical structure of the model based on spectral elements allows for application of state-of-the-art computing hardware most effectively and economically to produce the best prediction/simulation results with minimal expenditure of computing resources. The model has now been tested under various conditions beginning with the shallow water equations and ending with an AMIP style run that uses the initial conditions and physics used in the CAM2 AMIP experiments. For uniform resolution, the output of the model compares favorably with the published output from the corresponding CAM2 experiments. Integrations with local mesh refinement included indicate that while greater detail in the prediction of mesh refined regions, i.e., regional climate, is observed, the remaining course grid results are similar to

results obtained from a uniform grid integration of the model with identical conditions. The following figure demonstrates this result, showing the comparison of the model integration of total precipitation rate with and without LMR (local mesh refinement) over the North American region. For the complete story on the model's performance, see Baer, F., H. Wang, J. J. Tribbia, and A. Fournier, 2006: Climate modeling with spectral elements. *Mon. Wea. Rev.*, **134**, 3610–3624.



Variable resolution versus limited area modelling: perfect model approach

Michel Déqué and Samuel Somot
Centre National de Recherches Météorologiques, Météo-France.
42 avenue Coriolis F-31057 Toulouse Cédex 1, France, deque@meteo.fr

Whatever the power of computer available, climate modellers will find it insufficient to fulfill their needs in horizontal resolution in regional modelling. Two solutions are offered to make model less costly in computer time and core memory. The most widespread is nested modelling. It consists of using a low resolution global model to provide lateral boundary conditions to a limited area model (Denis et al., 2002). The alternative approach consists of keeping a global model, but with high resolution in a part of the globe and lower resolution elsewhere. Different numerical techniques can be used to this purpose. The Stretched Grid Model Intercomparison Project (SGMIP, Fox-Rabinowitz et al., 2005) presents and validates the different techniques.

The ARPEGE/IFS numerical core used at Météo-France and ECMWF proposes the two approaches in the same executable file. Indeed ALADIN is a special configuration of the model in which the sphere is replaced by a torus: in a part of the domain (one x- and one y-zonal band), no physical calculation is done but a smooth interpolation along the two directions is performed; on both sides of these two zones, the prognostic variables of the model are relaxed toward imposed lateral conditions. This method, first proposed by Haugen and Machenhauer (1993), allows to mimic the behaviour of a limited area grid point model with the same dynamics and physics as the driving model with a very competitive cost (only 27 rows in both x- and y-directions are not used for free atmospheric calculations). On the other hand, ARPEGE/IFS can be used with a stretched grid over the sphere: this is done daily in operational forecast, and has been used in climate modelling since Déqué and Piedelievre (1995).

In ARPEGE/IFS the two approaches compliment each other: ALADIN provides a further zoom in the stretched area of ARPEGE. In the present study, we want to compare the two approaches, so ARPEGE is constrained by the same data as ALADIN. This is why a grid point relaxation is introduced in ARPEGE outside the area where ALADIN is free to evolve. Figure 1 shows the free grid points in the two models in a configuration over Europe at 50 km resolution. Because of the projection techniques (stereographic for ARPEGE, Lambert for ALADIN) the two grids cannot exactly match.

If we want to be as model-independent as possible, the perfect model approach is preferable, as the only ingredient that produces the responses we will analyze is the change in geometry. We have thus produced, as forcing and verification data a global simulation with a uniform 0.5° grid (TL359) version of ARPEGE. This simulation uses monthly observed SST from 1979 through 2003.

From this simulation (named S0) 6-hourly data of the model variables are interpolated on both regional grids (stretched and limited area) and saved. Two additional simulations with ALADIN (named S1) and with ARPEGE in stretched geometry (TL159 stretching factor 2.5, named S2). Except the location of the grid points, all parameters are identical in the 3 simulations (time step, vertical levels, physics) or as far as possible (surface characteristics, horizontal diffusion). S1 and S2 also differ in the way the forcing is applied. In S1 model variables are exactly imposed at the boundary of the forcing zone, whereas the constraint is looser in S2 (6h relaxation for wind, 12h for temperature and surface pressure).

The results are analyzed for five variables (2m daily minimum and maximum temperature, 500 hPa height, mean sea-level pressure and precipitation) and two seasons. We compare the ability to reproduce the mean climate by root mean square differences (rmsd) S1-S0 and S2-S0 over a European domain (see figure 1) and the ability to reproduce the chronology of synoptic events by anomaly correlation coefficients (acc) S1 vs S0 and S2 vs S0 over the same domain. Table 1 shows rmsd and acc for the five fields on the domain. Calculation of rmsd is based on 25-year mean seasonal averages, whereas acc is based on daily values (6-hourly values for mslp and z500). One can see that the methods are comparable in winter. In summer, the stretched global model has a smaller temperature bias and a larger precipitation correlation.

References:

- Denis, B., R. Laprise, D. Caya and J. Côté, 2002: Downscaling ability of the one-way nested regional climate models: the big-brother experiment. *Clim. Dyn.*, 18, 627-646.
- Déqué, M. and J.P. Pielieuvre, 1995: High resolution climate simulation over Europe. *Clim. Dyn.*, 11, 321-339.
- Fox-Rabinovitz, M., J. Côté, B Dugas, M. Déqué, and J. L. McGregor, 2006: Variable resolution general circulation models: Stretched-grid model intercomparison project (SGMIP). *J. Geophys. Res.*, 111, D16104, doi:10.1029/2005JD006520.
- Haugen, J.E. and B. Machenhauer, 1993: A spectral limited-area model formulation with time-dependent boundary conditions applied to the shallow-water equations. *Mon. Wea. Rev.*, 121, 2618-2630.

		DJF					JJA				
		tn	tx	z500	mslp	prec	tn	tx	z500	mslp	prec
rmsd	S1-S0	0.7	0.5	8.6	0.7	0.4	1.0	1.4	21.3	0.5	0.5
	S2-S0	0.8	0.6	1.9	0.2	0.4	0.7	0.7	1.6	0.2	0.3
acc	S1:S0	0.86	0.90	0.97	0.97	0.76	0.62	0.71	0.90	0.90	0.38
	S2:S0	0.85	0.88	0.97	0.97	0.76	0.71	0.79	0.94	0.92	0.48

Table 1: Comparison of rmsd and acc for the limited area (S1) and the stretched (S2) models versus the high resolution model in winter and summer: daily minimum temperature (tn, K), maximum temperature (tx, K), 500 hPa height (z500,m) mean sea level pressure (mslp, hPa) and precipitation (mm/day).

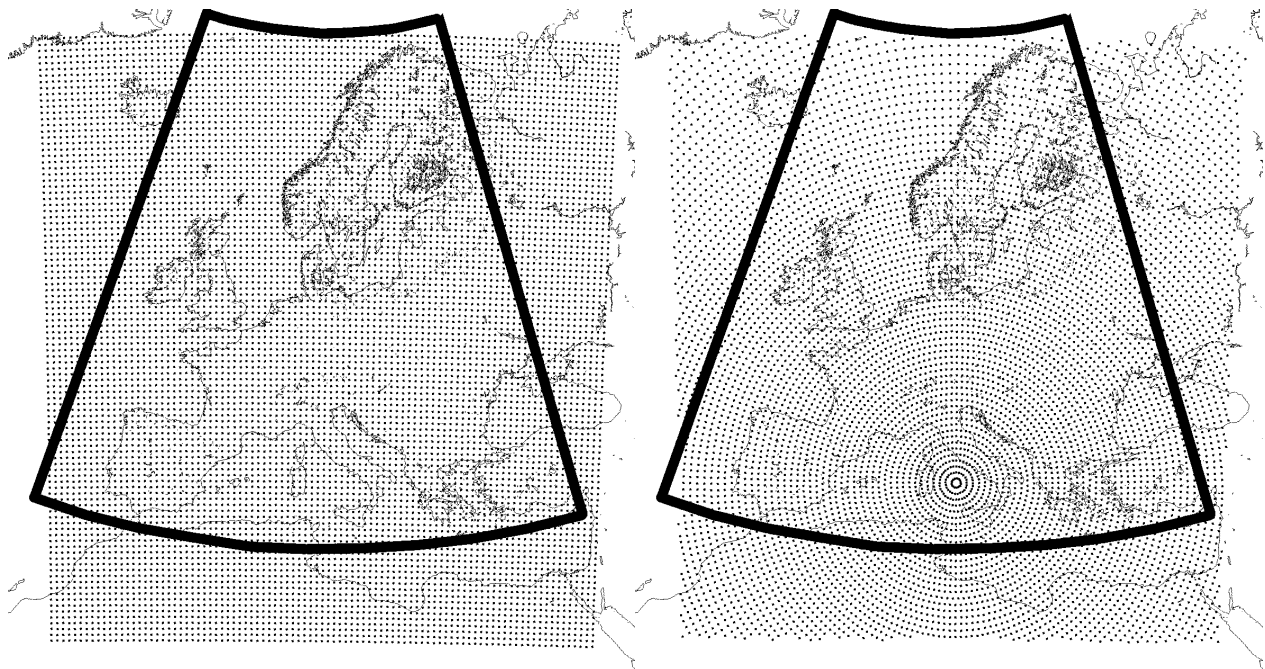


Figure 1: Grid points of ALADIN (left) and free part of ARPEGE (right); lat-lon domain of comparison

**Initial Results of the SGMIP-2
(Stretched-Grid Model Intercomparison Project, phase-2)**

Michael Fox-Rabinovitz, University of Maryland at College Park, U.S.A.,
Jean Côté and Bernard Dugas, Environment Canada, Canada,
Michel Déqué, Météo-France, France, and
John L. McGregor, CSIRO, Australia

Variable-resolution GCMs using a global stretched grid (SG) with enhanced resolution over the region(s) of interest have proven to be an established approach to regional climate modeling providing an efficient means for regional down-scaling to mesoscales. This approach has been used since the early-mid 90s by the French, U.S., Canadian, Australian and other climate modeling groups along with, or as an alternative to, the current widely-used nested-grid approach. Stretched-grid GCMs are used for continuous/autonomous climate simulations as usual GCMs, with the only difference that variable-resolution grids are used instead of more traditional uniform grids. The important advantages of variable-resolution SG-GCMs are that they do not require any lateral boundary conditions/forcing and are free of the associated undesirable computational problems. As a result, SG-GCMs provide self-consistent interactions between global and regional scales of motion and their associated phenomena, while a high quality of global circulation is preserved, as in uniform grid GCMs.

The first stage of the international project, SGMIP-1 (Stretched-Grid Model Intercomparison Project, phase-1), using variable-resolution SG-GCMs developed at the major centers/groups in Australia, Canada, France, and the U.S., has been successfully completed in 2005. The results of the 12-year (1989-1998) SGMIP-1 simulations are described by Fox-Rabinovitz et al. (2006a-c). The next stage of the international project, SGMIP-2 (phase-2) includes simulations for the extended period of 25 years (1979-2003). The major SGMIP-2 effort includes performing the experiments with: (a) SG-GCMs with the prime area of interest over the major part of North America and for an additional area of interest over Europe (both with $0.5^\circ \times 0.5^\circ$ regional resolution); (b) intermediate uniform grid (UG) GCMs at $1^\circ \times 1^\circ$ resolution, with the same number of global grid points as in the stretched grids; (c) fine uniform ($0.5^\circ \times 0.5^\circ$) resolution UG-GCMs, with the same global resolution as that of over the region of interest for the stretched grids (some model simulations are done for shorter periods due to computer resources available). The SGs for SG-SGMs (the SG-versions of the corresponding basic GCMs) are shown in Fig. 1.

These SGMIP-2 experiments provide the possibility for a comprehensive analysis of enhanced variable and uniform resolution GCMs and their unique high resolution multi-modes ensembles (MMEs) against observations and reanalyses. In-depth comparisons of enhanced variable and uniform (intermediate and fine) resolution GCMs are important for conducting a comprehensive investigation on the diversified impacts on decadal climate simulations due to enhanced regional and/or global model resolution, with the emphasis on the North American regional climate. The initial results of the SGMIP-2 climate simulations for the global domain and a major part of North America are available at the SGMIP web site: <http://essic.umd.edu/~foxrab/sgmip.html>

The SGMIP-2 products constitute a basis for collaboration with the NARCCAP (North American Regional Climate Change Assessment Program) and for potential collaboration with other regional model intercomparison projects (e.g. relevant European projects). The possibility of creating joint regional MMEs for nested and stretched grid models may be beneficial for the national and international regional climate modeling communities.

We conclude that over the region of interest: (a) SG-GCMs have overall smaller errors, than those of the intermediate ($1^\circ \times 1^\circ$) UG-GCMs; and (b) SG-GCMs and fine ($0.5^\circ \times 0.5^\circ$) UG-GCMs have overall similar errors. Also, SG-GCMs produce high quality global simulations.

SGMIP-2 was endorsed by the WMO/WCRP/WGNE at its annual meetings in October 2004, November 2005, and October 2006.

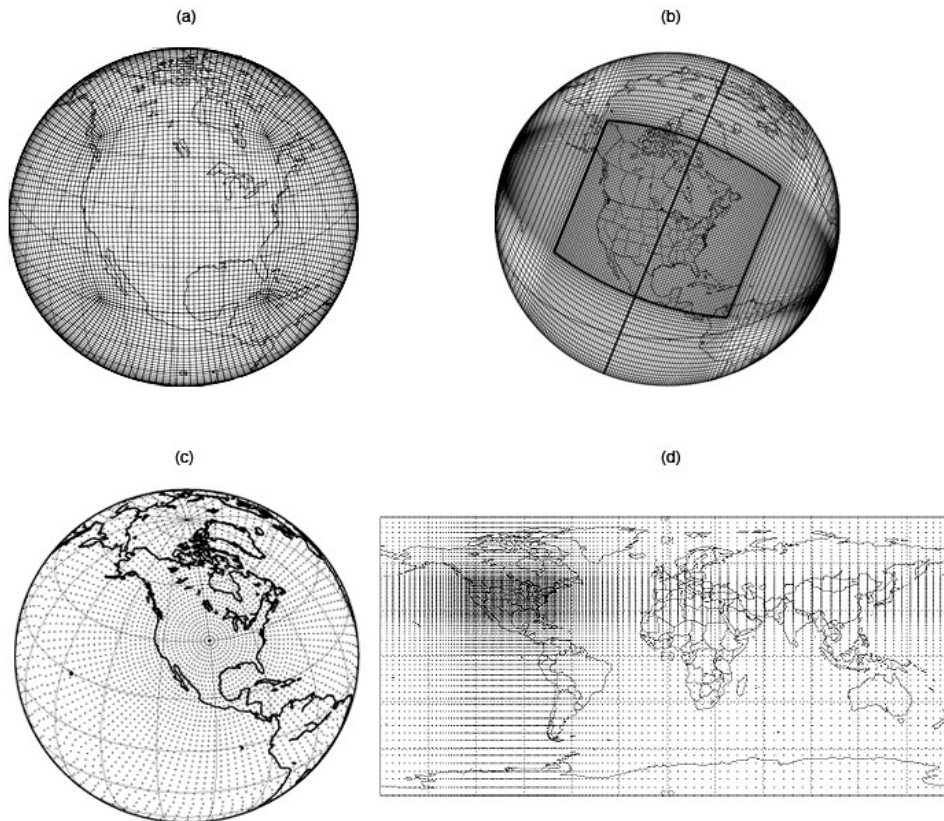


Fig. 1 SGMIP stretched grids with the area of interest over the major part of North America used in the following SG-GCMs: (a) C-CAM, CSIRO, Australia; (b) GEM, Environment Canada; (c) ARPEGE, Meteo-France; (d) GEOS, NASA/GSFC/UMD, U.S. Every other grid-line is shown.

References

1. Fox-Rabinovitz, M.S., J. Côté, B. Dugas, M. Déqué, and J.L. McGregor, 2006a: Variable resolution general circulation models: Stretched-grid model intercomparison project (SGMIP), *J. Geophys. Res.*, 111, D16104, doi:10.1029/2005JD006520.
2. Fox-Rabinovitz, M.S., J. Côté, B. Dugas, M. Déqué, J.L. McGregor, 2006b: Variable-Resolution GCMs for Regional Climate Modeling: Stretched-Grid Model Intercomparison Project (SGMIP), AGU Joint Assembly, Conference on Dynamical Regional Climate Modeling, May 22-26, 2006, Baltimore, MD.
3. Fox-Rabinovitz, M.S., J. Côté, B. Dugas, M. Déqué, J.L. McGregor, 2006c: Regional modeling with variable-resolution GCMs: Stretched-Grid Model Intercomparison Project (SGMIP), 2006 Workshop on the Solution of Partial Differential Equations on the Sphere, June 26-29 2006, Monterey CA.

Velocity reconstruction by radial basis functions in a triangular staggered C grid

Thomas Heinze, Tobias Ruppert

Deutscher Wetterdienst (DWD)

Kaiserleistr. 42, 63067, Offenbach, Germany

e-mail: thomas.heinze@dwd.de, tob_ruppert@gmx.net

Peter Korn

Max Planck Institut für Meteorologie (MPI-M)

Bundesstr. 53, 20146, Hamburg, Germany

e-mail: peter.korn@zmaw.de

Luca Bonaventura

MOX - Politecnico di Milano

P.zza Leonardo da Vinci 32, 20133, Milano, Italy

e-mail: luca.bonaventura@polimi.it

1 The ICON project

The ICON project is a joint development effort of MPI-M and DWD to achieve a unified climate and NWP model using geodesic grids with local grid refinement. The model under development in the ICON project will use the fully elastic, nonhydrostatic Navier-Stokes equations, which provide a framework that is sufficiently general for meteorological applications on most scales relevant to numerical weather prediction and climate simulation.

2 Velocity reconstruction

The proposed horizontal discretization uses the triangular staggered C grid approach. A full description of the horizontal discretization can be found in [2] and [3].

Vector radial basis function (RBF) interpolation is used to reconstruct a uniquely defined velocity field \vec{v} from the velocity components v_i normal to the cell sides.

The interpolation function \vec{s} for an arbitrary

point \vec{x} on the sphere is a linear combination of the unit vectors \vec{n}_i , that are normal to cell edges, multiplied by the RBF kernels Φ

$$\vec{s}(\vec{x}) = \sum_{j=1}^N c_j \cdot \Phi(\|\vec{x} - \vec{x}_j\|) \cdot \vec{n}_j \quad (1)$$

using N data points \vec{x}_j that satisfy the interpolation constraints

$$v_i = \vec{s}(\vec{x}_i) \cdot \vec{n}_i, \quad \forall i = 1, \dots, N \quad (2)$$

Hence the problem can be written as

$$v_i = \sum_{j=1}^N c_j \cdot \Phi(\|\vec{x}_i - \vec{x}_j\|) \cdot \vec{n}_j \cdot \vec{n}_i \quad \forall i = 1, \dots, N \quad (3)$$

and reduced to solve the linear system $\mathbf{A} \cdot \vec{c} = \vec{d}$ with

$$\begin{aligned} a_{ij} &= \Phi(\|\vec{x}_i - \vec{x}_j\|) \cdot \vec{n}_j \cdot \vec{n}_i \\ \vec{c} &= (c_1, \dots, c_N)^T \\ \vec{d} &= (v_1, \dots, v_N)^T \end{aligned}$$

The matrix \mathbf{A} is symmetric positive definite and the system can easily be solved by

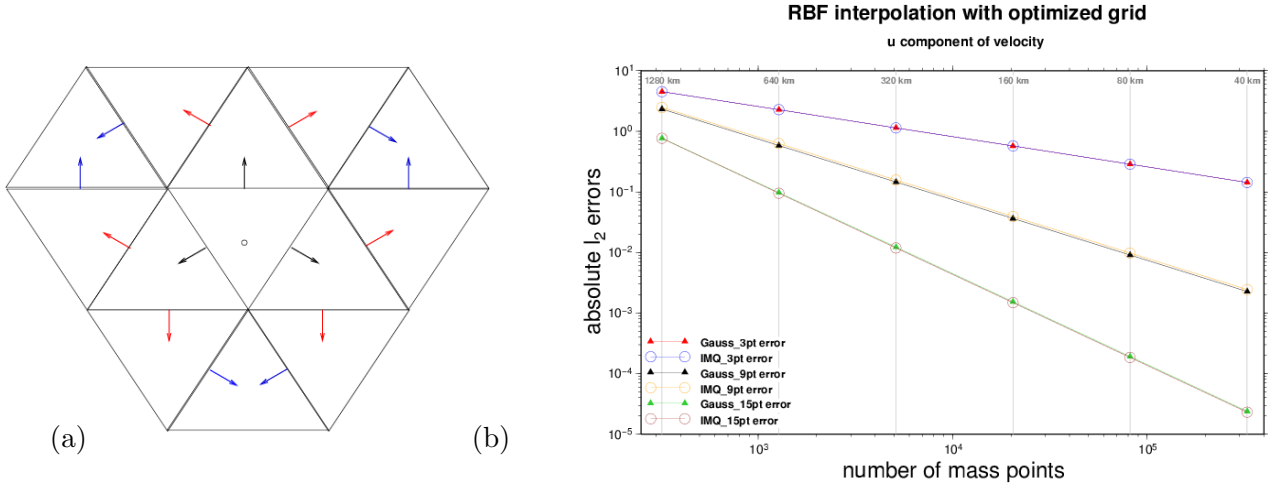


Figure 1: (a) 3 (black), 9 (red) and 15 (blue) point stencil (b) Convergence of zonal velocity component with different kernels and stencils

Cholesky decomposition.

In a triangular C grid setting the 3, 9 or 15 nearest edge centers are the natural choice for the N data points (see figure 1(a)).

Two kernels are investigated, Gaussian (GAU) and inverse multiquadric (IMQ).

$$\text{GAU: } \Phi(r) = e^{-\left(\frac{r}{\epsilon}\right)^2} \quad (4)$$

$$\text{IMQ: } \Phi(r) = \left(1 + \left(\frac{r}{\epsilon}\right)^2\right)^{-\frac{1}{2}} \quad (5)$$

where $r = \|\vec{x} - \vec{x}_j\|$ and ϵ is a scaling factor set to 0.9 (GAU) resp. 1 (IMQ) in the following example. More details of the mathematical background of the vector reconstruction by RBF can be found in [1].

Figure 1(b) shows a convergence plot for the zonal component of the reconstructed velocity. The error in the center of the triangles is calculated by comparing the interpolated velocity to the initial state of test case 6 of [4] (Rossby-Haurwitz wave number 4) in these points.

The outcome demonstrates that there are no relevant differences between the two RBF kernels, but the interpolation order depends on the chosen stencil. 1st order can be achieved by a 3 point, 2nd order by a 9 point and 3rd order by a 15 point stencil.

References

- [1] Jan Baudisch, Luca Bonaventura, Armin Iske, and Edie Miglio. Matrix valued radial basis functions for local vector field reconstruction: applications to computational fluid dynamic models. Technical Report MOX 75, Laboratory for Modeling and Scientific Computing MOX, Politecnico di Milano, Milan, Italy, 2006. 24 pp. Online available at <http://mox.polimi.it/it/progetti/publicazioni/quaderni/mox75.pdf>.
- [2] Luca Bonaventura, Luis Kornblueh, Thomas Heinze, and Pilar Rípodas. A semi-implicit method conserving mass and potential vorticity for the shallow water equations on the sphere. *International Journal of Numerical Methods in Fluids*, 47:863–869, 2005.
- [3] Luca Bonaventura and Todd Ringler. Analysis of discrete shallow water models on geodesic Delaunay grids with C-type staggering. *Monthly Weather Review*, 133:2351–2373, 2005.
- [4] David L. Williamson, John B. Drake, James J. Hack, Rüdiger Jakob, and Paul N. Swarztrauber. A standard test set for numerical approximations to the shallow water equations in spherical geometry. *Journal of Computational Physics*, 102(1):211–224, 1992.

Development of a hybrid terrain-following vertical coordinate for JMA Non-hydrostatic Model

Junichi Ishida

Numerical Prediction Division, Japan Meteorological Agency

e-mail : j-ishida@mth.biglobe.ne.jp

1 Introduction

The Japan Meteorological Agency (JMA) has been operating the JMA Non-hydrostatic Model (NHM) with a horizontal resolution of 5km since March 2006. The governing basic equations of NHM are the fully compressible equations and written in flux form. A time splitting method is used and the terms responsible for the sound and gravity waves are treated implicitly in the vertical direction and explicitly in the horizontal direction. The governing equations are transformed into a spherical curvilinear orthogonal coordinate and the vertical terrain-following coordinate (Gal-Chen and Somerville 1975).

The terrain-following transformation is linear and written in as follows:

$$z = \zeta + z_s \left(1 - \frac{\zeta}{z_T}\right),$$

where ζ is the transformed vertical coordinate, z_s is the surface height, and z_T is the model-top height.

This transformation has some advantages. A treatment of the lower boundary condition of this transformation is quite simple. Since ζ is linearly related to z , one-dimensional physical process such as atmospheric radiation and cumulus convection scheme will be implemented easily.

Since the coefficient of z_s of this transformation is not zero except at the model top, the constant- ζ levels are not flat even in the upper atmosphere and this non-orthogonal property would be a disadvantage. The horizontal pressure gradient term and the horizontal advection term are split into the horizontal and vertical derivative. Since the vertical grid spacing of NWP models is generally large in the upper atmosphere, the error of the vertical difference would cause errors of the pressure gradient force and the advection.

To reduce above disadvantage, a new hybrid vertical terrain-following coordinate which is based on the same approach as the η coordinate (Simmons and Burridge 1981) is implemented. It is transformed using following equation

$$z = \zeta + z_s f(\zeta).$$

The new transformation has the same advantages. As $f(\zeta)$ is getting close to zero, the constant- ζ levels become flat. Therefore the selection of the appropriate function can reduce the disadvantage. The function $f(\zeta)$ should satisfy $f(0) = 1$ and $f(z_T) = 0$ because of the boundary condition. The function $f(\zeta)$ must be second differentiable because the Christoffel's symbols require it and $f'(\zeta) > -1/z_s$ to make the transformation monotone.

2 Momentum Equations

The original momentum equations of NHM are as follows (Saito et al. 2006):

$$\frac{\partial U}{\partial t} + \frac{m_1}{m_2} \left(\frac{\partial P}{\partial x} + \frac{\partial G^{\frac{1}{2}} G^{13} P}{G^{\frac{1}{2}} \partial \zeta} \right) = -ADV_1 + R_1,$$

$$\frac{\partial V}{\partial t} + \frac{m_2}{m_1} \left(\frac{\partial P}{\partial y} + \frac{\partial G^{\frac{1}{2}} G^{23} P}{G^{\frac{1}{2}} \partial \zeta} \right) = -ADV_2 + R_2,$$

$$\frac{\partial W}{\partial t} + \frac{1}{m_3 G^{\frac{1}{2}}} \frac{\partial P}{\partial \zeta} = -ADV_3 + R_3.$$

Here U, V and W represent the momentum components and P the pressure perturbation. ADV and R are the advection terms and residual terms including the buoyancy term, respectively. Subscripts 1, 2 and 3 correspond to the x, y and ζ components, respectively. Symbols m_1 and m_2 are the map factors while m_3 is not a map factor but a constant introduced for definition of momentum. $G^{\frac{1}{2}}, G^{13}$ and G^{23} are metric tensors and given by

$$G^{\frac{1}{2}} = \frac{\partial z}{\partial \zeta}, \quad G^{\frac{1}{2}} G^{13} = -\frac{\partial z}{\partial x}, \quad G^{\frac{1}{2}} G^{23} = -\frac{\partial z}{\partial y}.$$

To introduce the hybrid vertical coordinate, above equations are rewritten by using tensor analysis as follows:

$$\frac{\partial U}{\partial t} + \frac{m_1}{m_2} \left(\frac{\partial P}{\partial x} + \frac{\partial G^{13} P}{\partial \zeta} \right) = -ADV_1 + R_1,$$

$$\frac{\partial V}{\partial t} + \frac{m_2}{m_1} \left(\frac{\partial P}{\partial y} + \frac{\partial G^{23} P}{\partial \zeta} \right) = -ADV_2 + R_2,$$

$$\frac{\partial W}{\partial t} + \frac{1}{m_3} \frac{\partial}{\partial \zeta} \left(\frac{P}{G^{\frac{1}{2}}} \right) = -ADV_3 + R_3.$$

Here, $G^{\frac{1}{2}}, G^{13}$ and G^{23} are written as follows:

$$G^{\frac{1}{2}} = 1 + z_s f'(\zeta),$$

$$G^{\frac{1}{2}} G^{13} = -f(\zeta) \frac{\partial z_s}{\partial x}, \quad G^{\frac{1}{2}} G^{23} = -f(\zeta) \frac{\partial z_s}{\partial y}.$$

Only the pressure gradient terms are modified by the introduction of the hybrid coordinate. The above equations correspond to the original equations if $G^{\frac{1}{2}}$ is independent of ζ . This means that the original equations are available for the original coordinate transformation (Gal-Chen linear transformation). Though the pressure gradient terms are modified, the computational cost of the hybrid coordinate is almost the same as that of the original coordinate.

3 Experiment results and conclusions

Idealised advection experiments with the original and hybrid coordinates are carried out to evaluate the computational error. The number of grid points is $301 \times 7 \times 50$ with a horizontal resolution of 1 km. A bell-shaped mountain with a height of 3000 m and a x-direction width of 50 km is placed at the centre of the domain. Initial potential temperature field and wind field are horizontally uniform and $\partial\theta/\partial z = 3$ K/km, $u = v = 0$ m/s ($z < 10000$ m) and $u = 2.5$ m/s and $v = 0$ m/s ($z > 12000$ m). A moisture mass with a width of 50 km and a thickness of 6000 m is placed 108 km west of the centre of the domain, at an altitude of 16000 m. This means that it will pass just over the mountain at the forecast time of 12 hours. The time step is 20 s and the time integration is carried out up to 24 hours. A fourth-order advection scheme with a flux correction scheme is used.

The following function is selected,

$$f(\zeta) = \frac{c \left\{ 1 - \left(\frac{\zeta}{z_T} \right)^n \right\}}{c + \left(\frac{\zeta}{z_T} \right)^n}, \quad c = \frac{\left(\frac{z_l + z_h}{2z_T} \right)^n}{1 - 2 \left(\frac{z_l + z_h}{2z_T} \right)^n},$$

where $z_T = 21600$, $z_l = 1000$, $z_h = 11000$ m and $n = 3$. The coefficient of z_s at the centre of the domain is shown in Fig. 1. The coefficient by the hybrid coordinate is almost zero at $z = 16000$ m while that by the original coordinate is about 0.3.

The result of the experiment with the original coordinate is shown in Fig. 2 and that with the hybrid coordinate is shown in Fig. 3. The moisture masses at $t = 0, 12$ and 24 h are drawn from left to right, respectively. The shape of the moisture mass in the hybrid coordinate is well-preserved while that in the original coordinate is remarkably deformed.

The hybrid vertical coordinate is implemented into NHM without the increase of the computational cost. This coordinate can be also used as the Gal-Chen vertical coordinate if $f(\zeta) = 1 - \zeta/z_T$. The hybrid coordinate and the new transformation function shown in above will be in operation in May 2007.

4 Acknowledgements

The author is grateful to Dr. Kazuo Saito of the Meteorological Research Institute and Mr. Tsukasa Fujita of JMA for their valuable comments and also thanks Mr. Tabito Hara and Mr. Kohei Aranami of JMA for their cooperation.

References

[1] Gal-Chen, T. and R. C. J. Somerville, 1975: On the use of a coordinate transform for the solution of the Navier-Stokes equation. *J. Comp. Phys.*, **17**, 209-228.

[2] Saito, K., T. Fujita, Y. Yamada, J. Ishida, Y. Kumagai, K. Aranami, S. Ohmori, R. Nagasawa, S. Kumagai, C. Muroi, T. Kato and H. Eito, 2006: The operational JMA Nonhydrostatic Mesoscale Model. *Mon. Wea. Rev.*, **134**, 1266-1298.

[3] Simmons, A. J. and D. M. Burridge, 1981: An energy and angular-momentum conserving vertical finite-difference scheme and hybrid vertical coordinates. *Mon. Wea. Rev.*, **109**, 758-766.

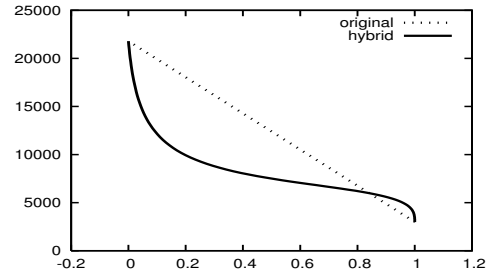


Figure 1: The coefficient of z_s by the hybrid transformation function (solid line) and the original transformation function (dotted line). The x-axis is the coefficient and the y-axis is the height.

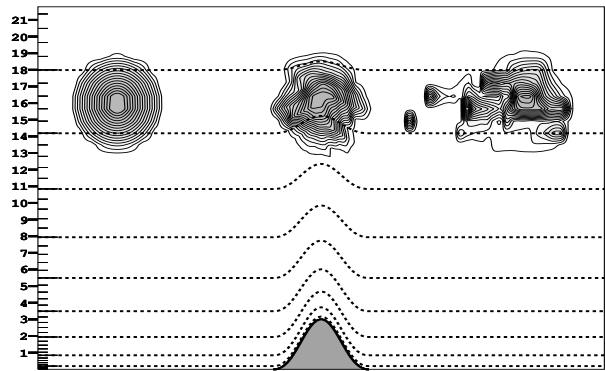


Figure 2: The result of the advection test with the original vertical coordinate. The moisture masses at $t = 0, 12$ and 24 h are drawn from left to right, respectively.

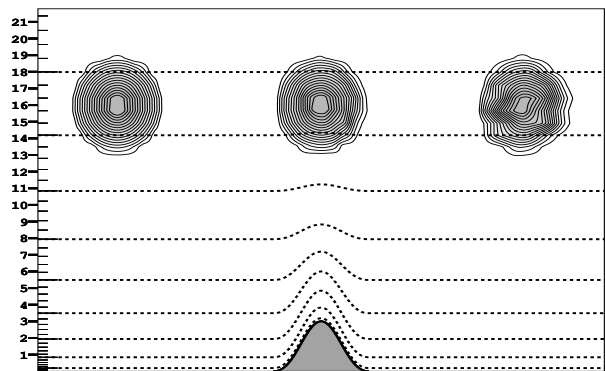


Figure 3: Same as in Figure 2 but with the hybrid vertical coordinate

Compound Parameterization for a Quality Control of Outliers and Larger Errors in NN Emulations of Model Physics

V. M. Krasnopolsky^{1,2}, email: Vladimir.Krasnopolsky@noaa.gov,

M. S. Fox-Rabinovitz¹, and A. Belochitski¹

¹Earth System Science Interdisciplinary Center, University of Maryland, USA

²SAIC at NCEP/NOAA, USA

1. Introduction

We have developed NN emulations of the long wave radiation (LWR) and short wave radiation (SWR) parameterizations [1,2,3] which are the most time consuming components of model physics of the National Center for Atmospheric Research (NCAR) Community Atmospheric Model (CAM).

The developed highly accurate NN emulations for LWR and SWR are two orders and one order of magnitude faster than the original/control NCAR CAM LWR and SWR, respectively [1,2,3]. The NN emulations use 50 neurons (NN50) for the LWR NN emulation and 55 neurons (NN55) for the SWR NN emulation in the hidden layer. They provide, if run *separately* at every model physics time step (1 hour), the speed-up of ~ 150 times for LWR and of ~ 20 times for SWR as compared with the original LWR and SWR, respectively [1,2,3].

The results of decadal climate simulations performed with NN emulations for both LWR and SWR, i. e., for the full model radiation block, have been validated against the parallel control NCAR CAM simulation using the original LWR and SWR. The almost identical results have been obtained for these two parallel 40-year climate simulations [4].

Larger errors and outliers (i.e. a few extreme errors) in NN emulation outputs have a very low probability (as will be shown in Fig. 1 below) and are distributed randomly in space and time. However, when decadal climate simulations are performed using NN emulations, the probability of obtaining larger errors may increase. As we learned from our experiments with NCAR CAM, the model was robust enough to filter out such randomly distributed errors, without their accumulation in time. However, for such a highly non-linear system as a climate model, it is desirable to introduce a quality control (QC) mechanism, which could predict and eliminate such errors during long-term model integration, not relying upon the robustness of a model that can vary significantly from one model to another. Such a mechanism would make our NN emulation approach more robust and generic. We introduced such a QC technique the combination of which with the NN emulation is called a compound parameterization (CP).

2. The Compound Parameterization Approach for Reduction of the Number and Probability of Larger Errors and Outliers in NN Emulations of Model Physics

CP consists of the following three elements: the original parameterization, its NN emulation, and a QC block. A nonlinear and effective QC design is based on training, for each NN emulation, an additional NN to specifically predict the errors in the NN emulation outputs for a particular input. During a routine climate model simulation with CP using NN emulation, the QC block determines at each time step of model integration and at each grid point whether the NN emulation or the original parameterization has to be used to generate physical parameters (i.e. parameterization outputs). Namely, when the NN emulation errors are too large for a particular grid point and time (i. e. if they exceed a predefined error

threshold) the original parameterization is used instead of NN emulation. In this case, inputs and outputs of the original parameterization can be saved to further adjust the NN emulation. Namely, after accumulating a sufficient number of these records, an adjustment of the NN emulation can be produced by a short retraining using the accumulated input/output records. Thus, the NN emulation becomes adjusted to the changes and/or new events/states produced by a complex climate model system.

An initial CP design was successfully tested for the NCAR CAM. An example of CP for SWR (see Fig.1) shows the comparison of

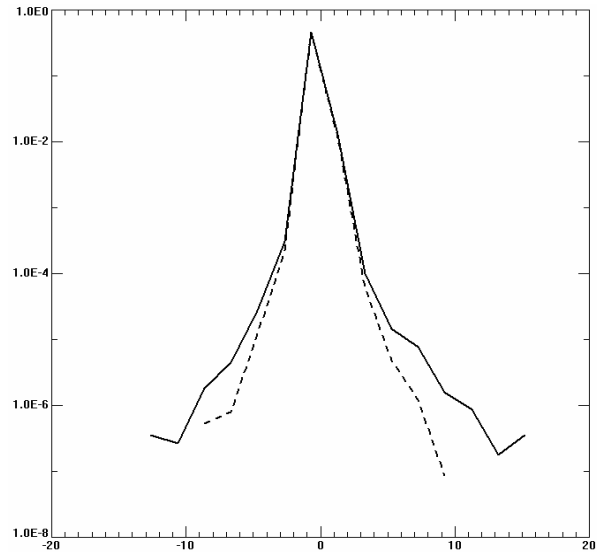


Fig.1. Probability density distributions of emulation errors for the SWR NN55 emulation (solid line) and for the SWR CP (dashed line). Both errors are calculated vs. the original SWR parameterization on the independent test set. Vertical axis is logarithmic.

two error probability density functions. It demonstrates the effectiveness of CP. Namely, application of CP reduces probability of medium and large errors by about an order of magnitude. Only the errors below the predetermined threshold are allowed during climate model simulation with CP. It is noteworthy that at each time step throughout the entire 40-year model simulation the NN emulation outputs were rejected by the QC and the original parameterization was used instead mostly for 0.05% - 0.1% but not more than for 0.4% - 0.6% of model grid points. Therefore, the computational performance of the model with NN emulation was practically not reduced and CP is still about 20 times faster than the original SWR parameterization.

3. Conclusions

A new CP approach is developed. It is applied to NN emulations of the SWR parameterization in NCAR CAM. When using CP for the highly non-linear climate model, practically all large and medium-large errors can be reliably controlled during long-term climate simulations.

REFERENCES

- [1] Krasnopolsky, V.M., M.S. Fox-Rabinovitz, and D.V. Chalikov, "New Approach to Calculation of Atmospheric Model Physics: Accurate and Fast Neural Network Emulation of Long Wave Radiation in a Climate Model", *Monthly Weather Review*, v. 133, No. 5, pp. 1370-1383, 2005.
- [2] Krasnopolsky V.M., and M.S. Fox-Rabinovitz, "Complex Hybrid Models Combining Deterministic and Machine Learning Components for Numerical Climate Modeling and Weather Prediction", *Neural Networks*, 19, 122–134, 2006.
- [3] Krasnopolsky V.M., and M.S. Fox-Rabinovitz, "A New Synergetic Paradigm in Environmental Numerical Modeling: Hybrid Models Combining Deterministic and Machine Learning Components", *Ecological Modelling*, v. 191, 5-18, 2006
- [4] Krasnopolsky, V.M., M. S. Fox-Rabinovitz, and A. Belochitski, "Accurate and Fast Neural Network Emulation of Full, Long- and Short Wave, Model Radiation Used for Decadal Climate Simulations with NCAR CAM", 19th Conference on Climate Variability and Change/ Fifth Conference on Artificial Intelligence Applications to Environmental Science, 87th AMS Annual Meeting, San Antonio, TX , 14—18 January 2007, J3.3, CD-ROM.

AGCM parallel realization on cluster.

V.P. Parkhomenko

Computing Centre of the Russia Academy of Sciences

Vavilov Str. 40 Moscow 119967 Russian Federation

One of the purposes of the work is to analyze components of AGCM algorithm and their parallel performance depending on computing program efficiency, to find bottlenecks that hinder the parallel scalability of the code, and use better algorithms and more efficient parallel implementation strategies to maximize the performance of the AGCM code on scalable parallel systems.

Computing Centre (CC) AGCM uses uniform 72 on longitude and 46 on a latitude horizontal grid for single processor computer. Program was modified for high performance cluster. An analysis is presented of the primary factors influencing the performance of a parallel implementation of AGCM on distributed-memory, cluster computer system. Several modifications to the original parallel AGCM code aimed at improving its numerical efficiency, load-balance code performance are discussed. The climate model includes the atmospheric block realized on the basis of AGCM with physical processes parameterization. Versions of model with fine spatial grid and the ocean general circulation model are developed. Interaction between blocks is carried out in an interactive mode. The model has rather coarse spatial grid, however relatively low computing expenses allows to investigate mechanisms and ways of parallelization for research their efficiency and definition of bottlenecks.

Domain decomposition in horizontal directions is used in parallel realization of the model. This choice is based on the fact that vertical processes strongly connect grid points that make parallelization by less effective in a vertical direction, and that the number of grid points in a vertical direction is usually small. Each grid cell is rectangular area which contains all points of a grid in a vertical direction.

There are two major components of the code: AGCM Dynamics, which computes the evolution of the fluid flow governed by the primitive equations by means of finite-differences, and AGCM Physics, which computes the effect of processes not resolved by the model's grid (such as convection on cloud scales) on processes that are resolved by the grid. The results obtained by AGCM Physics are supplied to AGCM Dynamics as forcing for the flow calculations. The AGCM code uses a three dimensional staggered grid for velocity and thermodynamic variables (potential temperature, pressure, specific humidity, ozone, etc.). The AGCM Dynamics itself consists of two main components: a spectral filtering part and the actual finite difference calculations. The filtering operation is needed at each time step in regions close to the poles to ensure the effective grid size there satisfies the stability requirement for explicit time difference schemes when a fixed time step is used throughout the entire spherical finite-difference grid.

In this case there are basically two types of interprocessor data exchanges. Data exchanges are necessary between logically next processors (units) at calculations of final differences; the removed data exchanges are necessary to carry out operations of spectral filtering, in particular. It is found that implementation of a load-balanced Fourier algorithm results in a reduction in overall execution time of approximately 40% compared to the original algorithm.

The basic part of computing expenses of AGCM is connected with the Dynamics component and the Physics component, with the excluded procedures of input-output. These

procedures are carried out only once whereas the main components are calculated repeatedly on time and dominate on expenses of performance time. Comparing the two modules in the main body, we can see the Dynamics part is dominant in cost especially on large numbers of nodes. Furthermore, timing analysis on the Dynamics part indicates that the spectral filtering is a very costly component with poor scalability to large number of nodes

The physical block of AGCM carries out local calculations without interprocessor exchanges. Distribution of computing loading in the physical block changes in time and space at the account of model and non-uniformity of loading of processors achieves 50 %. The amount of calculations in each grid point is defined by several factors: time of day, distribution of clouds, presence cumulus convection. Difficulty of maintenance of uniformity of loading of the physical block is unpredictability of distribution of clouds and distributions cumulus convection. The estimation of each processor loading is required before realization of the effective loading balancing. Preliminary results of the application of a load-balancing scheme for the Physics part of the AGCM code suggest additional reductions in execution time of 15-20% can be achieved.

The analysis of some factors influencing performance of AGCM parallel realization on the cluster is submitted. Some updating of an initial parallel AGCM code, directed on improvement of its computing efficiency, balance of processors loading are discussed. It is revealed, that performance of the balanced loading of algorithm of spectral smoothing provides reduction of performance time approximately on 40 %, in comparison with initial algorithm. Test calculations on high-efficiency cluster are carried out.

Realization of the parallel program for various ways of splitting of global area on processors in climatic model is carried out. Updating of the time integration numerical scheme for an opportunity of realization of parallel calculations of dynamics and physics blocks with an estimation of computation efficiency is carried out. The analysis shows, that results of calculations under the modified scheme yields satisfactory results and its application is possible. In the scalar program physics block run time takes 38%, and dynamics block run time - 62%. It means that parallel program acceleration in one and a half time can be achieved. Offered procedure is used together with parallel computations of dynamics and physics blocks on the basis of global area decomposition. It allows to optimize loading of processors and to increase program efficiency. Results of application of loading balance of the physics block of AGCM enable additional reduction of running time on 15-20 %. Other opportunity of method application is a complication of the physics block without increasing of total computational time.

This work is supported by RFFI.

References

- Wehner, M.F., A.A. Mirin, P.O. Eltgroth, WP. Dannevik, C.R. Mechoso, J. Farrara, J.A. Spahr, Performance of a Distributed Memory Finite-Difference Atmospheric General Circulation Model, *Parallel Computing* 21, 1655-1675, 1995.
- V.P. Parkhomenko Parallel Atmospheric General Circulation Model Code Analysis and Optimization. Research activities in atmospheric and oceanic modelling. World Meteorological Organization Geneva Switzerland 2005, V. 35, p. 3.19 – 3.20.

SHALLOW WATER EQUATIONS WITH CHEMICAL TRANSPORT

Janusz A. Pudykiewicz, Environment Canada, RPN, e-mail: Janusz.Pudykiewicz@ec.gc.ca

The main requirements for the accurate numerical technique for solving the fully coupled system of atmospheric dynamics and chemistry include stability for stiff systems, monotonicity, mass conservation, small numerical diffusion, and flexibility with respect to the selection of horizontal discretization. The selection of the optimum method satisfying all these requirements is not easy and it requires extensive studies of both analytical and numerical nature. The majority of these studies could be accomplished analyzing a relatively simple set of shallow water equations coupled to a set of reaction-advection-diffusion equations

$$\frac{\partial \mathbf{v}}{\partial t} + (\zeta + f)(\mathbf{k} \times \mathbf{v}) = -\nabla(g h + \frac{\mathbf{v}\mathbf{v}}{2}) \quad (1)$$

$$\frac{\partial h^*}{\partial t} + \nabla(h^* \mathbf{v}) = 0. \quad (2)$$

$$\frac{\partial \varphi^k}{\partial t} = -\nabla \mathbf{v} \varphi^k + \nabla \mathbf{K} \nabla \varphi^k + F_c^k(\varphi^1, \dots, \varphi^{N_s}), \quad (3)$$

where \mathbf{v} is the velocity field on the sphere, ζ is the vertical component of vorticity, f is the Coriolis parameter, h^* is the geopotential height, h_s is the surface height, \mathbf{k} is the unit vector normal to the sphere, and g is the gravity acceleration, φ^k is the k^{th} scalar field; $k = 1, \dots, N_s$, N_s is number of scalar fields, \mathbf{K} is the diffusion tensor, and F_c^k are the functions describing the interactions between scalar fields. In a general case, F_c^k can be written as $\alpha_{klm} \varphi^l \varphi^m + \beta_{kl} \varphi^l$, where α_{klm} and β_{kl} are the kinetic coefficients. The system of equations (1)-(3) is discretized on a geodesic icosahedral grid (Fig. 3) using a finite volume method developed originally for scalar conservation laws (Pudykiewicz, 2006). The methodology employed is based on the concept of semidiscretization; first the operators on the right hand sides of (1)-(3) are approximated and then, the resulting set of the Ordinary Differential Equations (ODEs) is solved using the appropriate time stepping algorithm. Depending on the stiffness of the system, the time integration is performed either with the 4th order Runge-Kutta scheme or with the Rosenbrock solver. The performance of the numerical technique for the coupled set of equations (1)-(3) is assessed using the initial conditions defining the Rossby-Haurwitz wave number 12 (Williamson et al., 1991) with the chemistry described by the Brusselator system (Prigogine and Lefever, 1968). This experimental setting is interesting from the point of view of the interaction of dynamics and chemistry because the tracer filamentation by the Rossby wave (Pierrehumbert, 1991) is coupled in a complex manner with the nonlinear chemistry. The chemical terms on the right hand side of (3) used in the study can be described as

$$F_c^1 = k_1 a - (k_4 + k_2 b) \varphi^1 + k_3 (\varphi^1)^2 \varphi^2 \quad (4)$$

$$F_c^2 = k_2 b \varphi^1 - k_3 (\varphi^1)^2 \varphi^2 \quad (5)$$

The parameters of the chemical system were selected as follows: $\mu_1 = 0.7 \times 10^5 [\text{sec}^{-1}]$, $\mu_2 = 2\mu_1$, $k_i = 1.16 \times 10^{-5} [\text{sec}^{-1}]$ (for $i = 1, \dots, 4$), $a = 2$, $b = 5$. The main property of the reaction-diffusion system with such parameters is the tendency to develop patterns in form of the stripes and belts. The effect of the interaction of the pattern formation with the stretching and folding of the material surfaces by the evolving unstable Rossby wave is depicted in Figs. 4-6 (initial conditions for φ^1 is shown in Fig. 1; $\varphi^2 = \varphi^1 + ((b/a) - a)$). The main conclusion from the experiment investigating numerical solver in a complex setting of a fully interactive scheme involving nonlinear dynamics and chemistry is that the system is able to develop fine structures resulting both from chemistry (pattern formation) and dynamics (filamentation) without numerical noise. Despite the very fine structures of the tracer filaments, the advected chemical tracer fields remained positive definite during the prolonged numerical integration of (1)-(3) on icosahedral geodesic grid.

REFERENCES

- [1] Pierrehumbert R. T., 1991: Chaotic Mixing of Tracer and Vorticity by Modulated Traveling Rossby Waves. *Geophysical and Astrophysical Fluid Dynamics*, **58**, 285-320.
- [2] Prigogine I. and R. Lefever, 1968: Symmetry-Breaking Instabilities in Dissipative Systems. *J. Chem. Phys.*, **48**, 1695-1700.
- [3] Pudykiewicz J., 2006: Numerical solution of the reaction–advection–diffusion equation on the sphere. *J. Comp. Phys.*, **213**, 358.
- [4] Williamson D. L., J. B. Drake, J. J. Hack, R. Jakob, and P. N. Shwartzrauber, 1992: A Standard Test Set for Numerical Approximations to the Shallow Water Equations in Spherical Geometry. *J. Comp. Phys.*, **102**, 211.

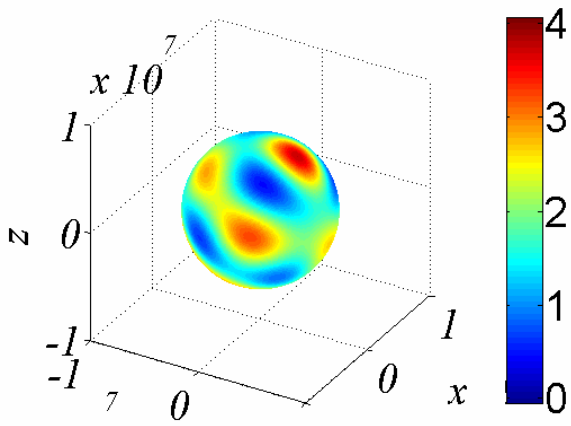


Fig. 1 The initial condition for the first chemical field

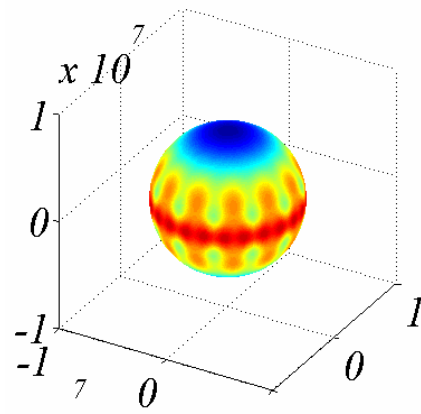


Fig. 2 The geopotential field after 24 hrs.

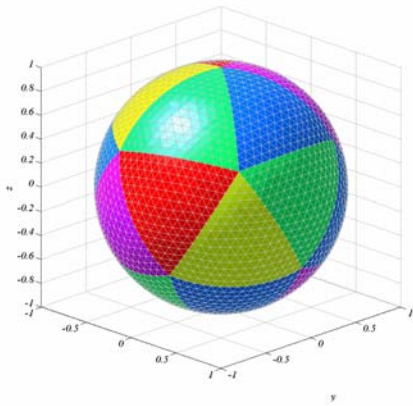


Fig. 3 The geodesic grid obtained after 4 divisions of the original icosahedron; calculation shown in Figs. 4-6 were performed on grid obtained after 6 divisions

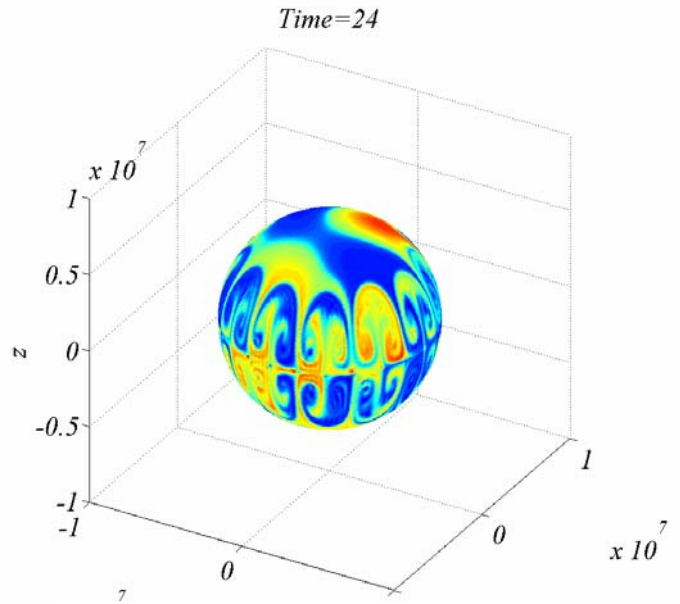


Fig. 4 First chemical field after 24 hours of integration

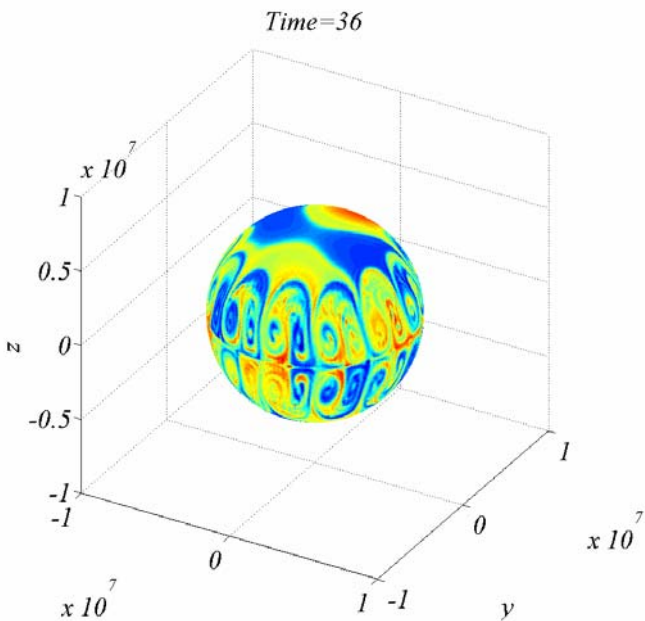


Fig. 5 First chemical field after 36 hours of integration

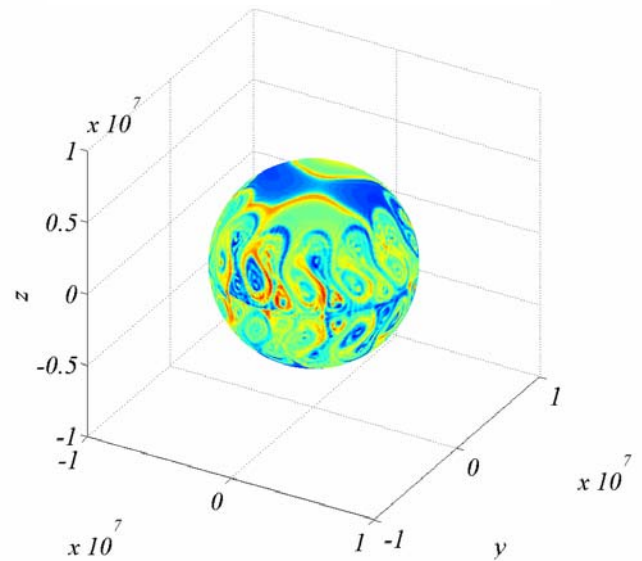


Fig. 6 First chemical field after 48 hours of integration

Improvements in the Scalability of the NASA Goddard Multiscale Multicomponent Modeling Framework for Hurricane Climate Studies

Bo-Wen Shen¹, Wei-Kuo Tao², and Jiun-Dar Chern³

¹UMCP/ESSIC, ²NASA/GSFC, ³UMBC/GEST

bo-wen.shen.1@gssc.nasa.gov, wei-kuo.tao.1@gssc.nasa.gov, jiun-dar.chern.1@gssc.nasa.gov

1. Introduction:

The 2004 and 2005 Atlantic hurricane seasons were the most active in recorded history, but the 2006 season was not as active as predicted. Therefore, a challenging research topic is how to improve our understanding of hurricane inter-annual variability and the impact of climate change on hurricanes. To address it with numerical models, we need to improve hurricane simulations on a global scale. Paired with the substantial computing power of the NASA Columbia supercomputer, the newly-developed multi-scale modeling framework (MMF, Tao et al. 2007) at the NASA Goddard Space Flight Center shows potential for the related studies. The Goddard MMF consists of two NASA state-of-the-art modeling components: the finite-volume General Circulation Model (fvGCM, Lin et al. 2004) and the 2-D version of the Goddard Cloud Ensemble Model (GCE, Tao and Simpson 1993; Tao et al. 1993). While the fvGCM has shown remarkable capabilities in simulating large-scale flows and thus hurricane tracks (Atlas et al. 2005; Shen et al. 2006a,b), the GCE is well known for its superior performance in representing small cloud-scale motions and has been used to produce more than 90 referred journal papers (e.g., Lang et al. 2003; Tao et al. 2003). Preliminary results with the MMF are encouraging, showing a positive impact on simulations of large-scale flows via the feedback of resolved convection by the GCEs. Among them is the improved simulation of the Madden-Julian Oscillation, which could potentially improve long-term forecasts of tropical cyclones. Since a higher resolution (e.g., 1 degree) fvGCM and 3-D GCE are desired in the MMF for hurricane (long-term) climate studies, computational issues in the Goddard MMF (e.g., limited scalability) need to be addressed.

2. The Goddard MMF:

The Goddard MMF consists of the fvGCM at a $2^{\circ} \times 2.5^{\circ}$ resolution and 13,104 2D GCEs, each of which is “embedded” within one grid point of the fvGCM. Currently, only thermodynamic feedback between the fvGCM and the GCEs is implemented. While the time step for the individual GCE is ten seconds, the fvGCM-GCEs coupling interval is one hour at this resolution. Under this configuration, 95% or more of the total wall-time for running the MMF is spent on the GCEs. Thus, wall-time could be significantly reduced by efficiently distributing the large number of GCEs over a massive number of processors on a supercomputer.

During the past several years, an SPMD (single program multiple data) parallelism has been implemented in both the fvGCM and GCE with good parallel efficiency separately (Putman et al. 2005; Juang et al. 2007). While the fvGCM has a hybrid MPI-OpenMP parallelism, the GCE has a 2D domain decomposition using MPI-1. Since it would require a tremendous effort to implement an OpenMP parallelism into the GCE or extend the 1D domain decomposition to 2D in the fvGCM, the MMF only inherited the fvGCM’s 1D MPI parallelism. This limited the MMF’s scalability, and thereby posed a challenge for increasing the fvGCM’s resolution and/or extending the GCE’s dimensions from 2D to 3D.

3. A Revised Parallelism Implementation:

To overcome the aforementioned limitation, we propose a different strategic approach to coupling the GCEs to the fvGCM. From a computational perspective, we should completely forget about the concept of “embedded GCEs”, which restricts our view on the data parallelism of the fvGCM. Instead, we could view the 13,104 GCEs as a *meta global GCE* (mgGCE) in a *meta gridpoint system*, which includes 13,104 grid points (Figure 1). This grid system, which is not limited to any specific grid system, is assumed to be the same as the latitude-longitude grid structure in the fvGCM for convenience. With this concept in mind, either the fvGCM or mgGCE can have its own scaling properties. Thus, we could substantially reduce the execution wall-time by deploying a highly scalable mgGCE, and/or coupling the mgGCE with the fvGCM using an MPMD (multiple programs multiple data) parallelism.

Data parallelism in the mgGCE is indeed a task parallelism, which distributes 13,104 GCEs among processors. As a cyclic lateral boundary condition is used in each GCE, the mgGCE has no ghost region in the meta grid system, so the mgGCEs with a 2D domain decomposition can be scaled “embarrassingly”. The major overhead in the MMF occurs in data redistribution (or regridding) between the fvGCM and the mgGCE. Under this new concept, the grid inside each GCE becomes a *child grid* (or sub-grid) with respect to the parent (meta) grid. Since an individual GCE

can still be executed with its native 2D-MPI implementation in the child grid-point space, this second level of parallelism can greatly expand the number of CPUs. Potentially, the final mgGCE and the coupled MMF as well could be scaled at a multiple of 13,104 CPUs. Another advantage of the mgGCEs is to permit the adoption of the idea of land-sea masks in a land model. For limited computing resources, we can create a cloud-mask file to specify limited regions where GCEs will be running, thereby possibly balancing computational loads. A sophisticated mgGCE implementation with the cloud-mask file will enable one to choose a variety of GCEs (2D vs. 3D, bulk vs. bin microphysics) depending on geographic location.

Currently, a prototype MMF with the mgGCE idea has been successfully implemented. The technical approaches are briefly summarized as follows: (1) a master process allocates a shared memory arena for data redistribution between the fvGCM and the mgGCE by calling the Unix *mmap* function; (2) the master process spawns multiple (parent) processes with a 1-D domain decomposition in the y direction by a series of Unix *fork* system calls; (3) each of these parent processes then forks several child processes with another 1-D domain decomposition along the x direction; (4) data gathering in the mgGCE is done via data communication along the x and then y directions; (5) synchronization is implemented with the atomic *__sync_add_and_fetch* function call on the Columbia supercomputer. While steps (1), (2), and (5) were previously used in single-component models by Taft (2001), we extend this methodology to our multicomponent modeling system. Figure 2 shows very promising scalability up to 364 CPUs, giving a super-linear speedup as measured by the production run with 30 CPUs.

4. Concluding Remarks:

Improving our understanding of hurricane inter-annual variability and the impact of climate change (e.g., doubling CO₂ and/or global warming) on hurricanes brings both scientific and computational challenges to researchers. The newly-developed MMF (Tao et al. 2007) and the substantial computing power of the NASA Columbia supercomputer show promise in studying this topic. In this article, we discuss the computational issues in hurricane climate studies with the MMF, and propose a revised methodology to improve the MMF's performance and scalability. A prototype of a revised MMF, which allows data redistribution between the fvGCM grid space and the mgGCE meta grid space, is being implemented with remarkable scalability. This proof-of-concept approach encourages us to implement a more sophisticated modeling coupler to solve complex problems with advanced computing power.

As the meta grid system in the mgGCE is no longer bound to the fvGCM's grid system, we could avoid the performance issues of a latitude-longitude grid system by implementing a quasi-uniform grid system (such as a cube grid or geodesic grid) in the mgGCE. Finally, as the MMF's major computing is done in the mgGCE, which has no ghost points, we envision the next version of the MMF with the mgGCE to be a good candidate for the meta- (grid-) computing like the SETI@home project. Namely computations in the mgGCE could be distributed among available (personal) computers connected by the Internet.

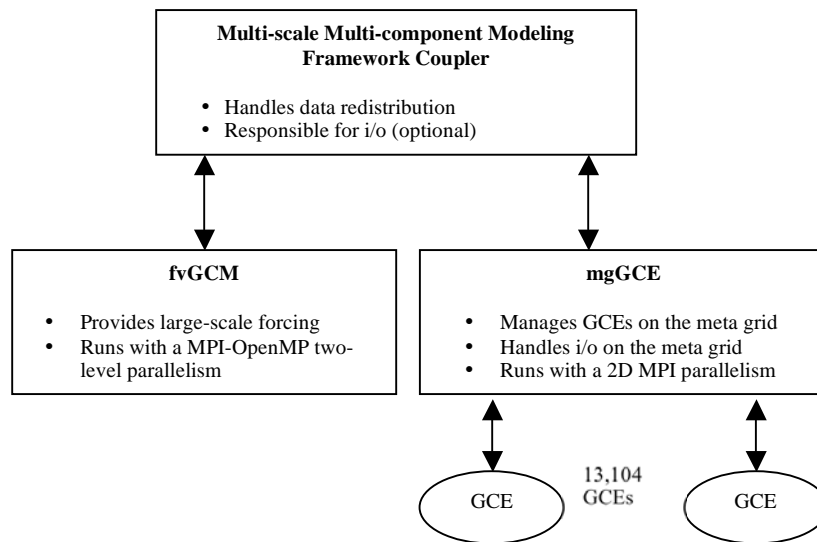


Figure 1 (top): Schematic diagram of the meta-global GCE and the improved MMF coupler.

Figure 2 (right): Scalability of the Goddard MMF.

References:

- Atlas et al. 2005, *GRL*, **32**, L03801.
- Juang et al. 2007, *TAO*, in press.
- Lang et al. 2003, *J. Appl. Meteor.* **42**, 505-527.
- Lin et al 2004, *CISE*, **6(1)**, 29-35.
- Putman et al. 2005, *IJHPCA*, **19**, 213-223.
- Shen et al 2006a: *GRL*, **33**, L05801.
- Shen et al 2006b: *GRL*, **33**, L13813.
- Taft, J. R. 2001, *P.C.*, **27** (4), 521-536
- Tao and Simpson, 1993, *TAO*, **4**, 19-54.
- Tao et al. 1993, *JAS*, **50**, 673-690.
- Tao et al. 2003, *JAS*, **60**, 2929-2956.
- Tao et al. 2007, *JGR*, submitted.

